Cancer Cell, Volume *29*

Supplemental Information

Single-Cell Phosphoproteomics Resolves Adaptive Signaling Dynamics and Informs Targeted Combination Therapy in Glioblastoma

Wei Wei, Young Shik Shin, Min Xue, Tomoo Matsutani, Kenta Masui, Huijun Yang, Shiro Ikegami, Yuchao Gu, Ken Herrmann, Dazy Johnson, Xiangming Ding, Kiwook Hwang, Jungwoo Kim, Jian Zhou, Yapeng Su, Xinmin Li, Bruno Bonetti, Rajesh Chopra, C. David James, Webster K. Cavenee, Timothy F. Cloughesy, Paul S. Mischel, James R. Heath, and Beatrice Gini

Supplemental Data

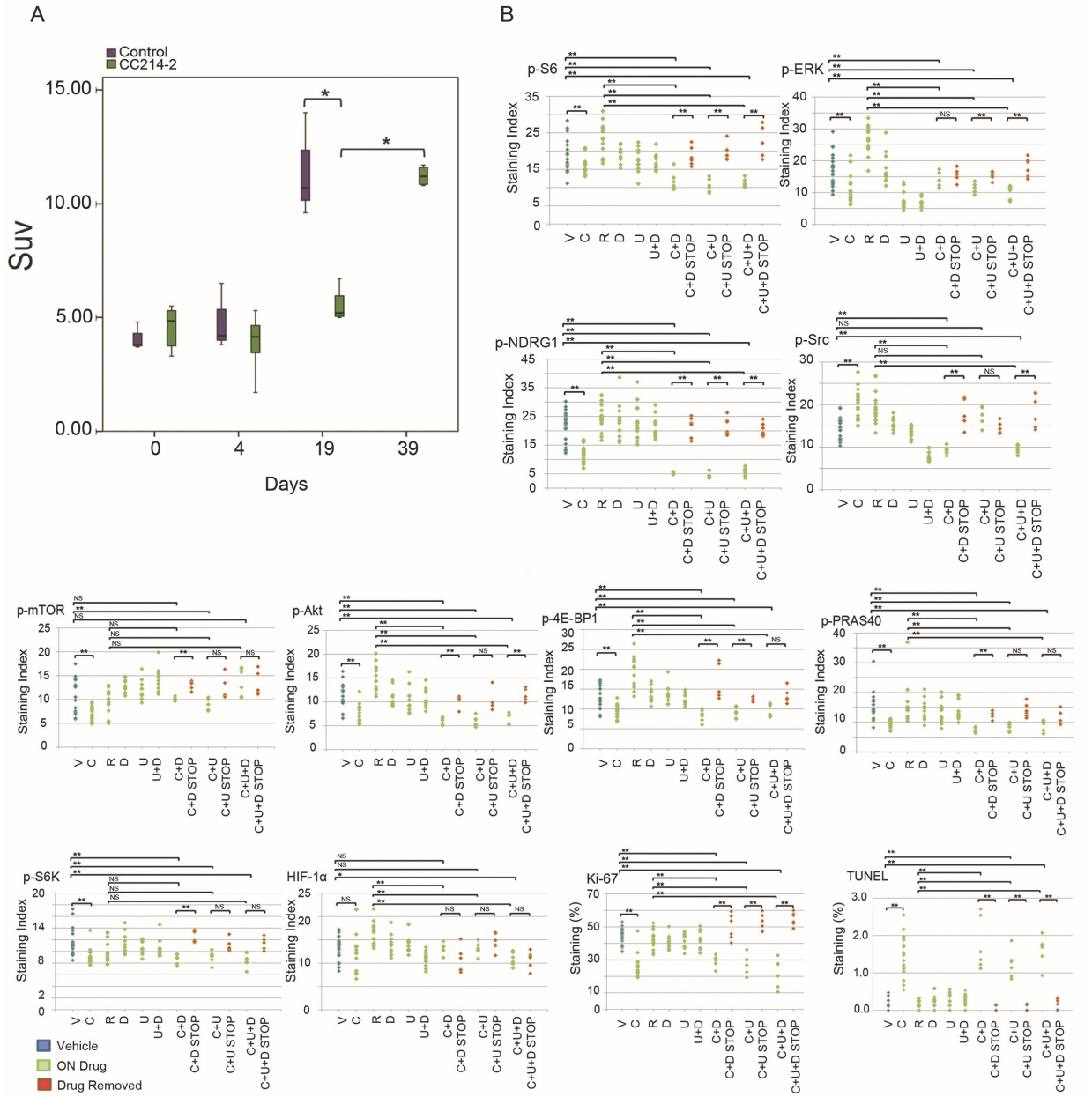

Figure S1, related to Figures 1 and 5. Characterization of GBM39 PDXs. (A) ^{18}F-FDG PET on GBM39 xenografts with statistical analysis of the Standardized Uptake Value (Suv) registered by imaging; *p<0.05 (One-way ANOVA and Student's T-test with Bonferroni correction; n= 4 for each box plot). Each box plot is determined by the 25th and 75th percentiles of the Suv and the whiskers are determined by the 5th and 95th percentiles of the Suv, with the median Suv value denoted by the horizontal line in the box. **(B)** IHC staining on GBM39 xenograft samples with statistical analysis of the quantitative IHC graphs for the mTOR, ERK, Src and hypoxia biomarkers and functional response markers (quantitative value averages were listed in Table S1; C: CC214-2 responsive samples; R: CC214-2 resistant samples; D: dasatinib; U: U0126; stop: xenografts collected after interruption of the treatments). Each data point represents a signal index extracted from a specific section field of a xenograft sample in a treatment group. Three independent section fields were captured for each xenograft and multiple xenografts were used in each treatment group (the number of xenografts used in each group was listed in the Experimental Procedures). **p<0.005; N.S., Not Significant (one-way ANOVA and Student's T-test with Bonferroni correction).

Table S1, related to Figures 1 and 5, IHC quantification of the GBM39 xenograft stains.

	Ki-67 (%)	Tunel (%)	p-Src	p-ERK	HIF-1α	p-mTOR
vehicle	43.44	0.13	14.82	17.13	13.40	11.25
C	25.96	1.46	19.98	11.49	12.71	7.25
R	42.69	0.14	19.32	26.43	16.23	9.70
D	40.37	0.22	15.46	17.24	13.89	12.74
U	42.26	0.23	13.38	7.53	14.25	11.92
U+D	41.80	0.26	7.75	6.96	10.91	14.56
C+D	29.30	1.75	9.26	13.75	13.08	10.02
C+D DR	49.91	0.07	18.61	15.05	10.59	12.90
C+U	27.53	1.23	16.77	11.11	13.09	9.13
C+U DR	52.60	0.10	14.57	15.35	14.52	12.12
C+U+D	22.05	1.61	9.45	10.13	10.88	13.74
C+U+D DR	54.84	0.17	18.60	17.95	10.78	12.99

	p-S6K	p-S6	p-4E-BP1	p-Akt	p-NDRG1	p-PRAS40
vehicle	11.50	18.34	12.86	11.02	21.29	15.42
C	8.78	15.90	9.48	7.51	11.94	9.12
R	9.98	23.31	19.28	14.86	25.01	16.03
D	11.24	18.98	13.56	10.67	23.15	14.17
U	10.60	17.23	13.74	10.39	23.45	14.01
U+D	10.39	16.91	12.53	10.76	21.53	13.70
C+D	8.68	11.76	8.36	5.82	5.06	7.30
C+D DR	12.62	18.55	17.60	10.20	21.37	12.61
C+U	9.03	10.56	9.09	5.88	4.72	8.47
C+U DR	10.93	19.59	12.52	9.69	21.70	13.97
C+U+D	8.55	11.24	9.73	6.34	5.69	9.08
C+U+D DR	11.60	21.78	13.22	11.70	20.53	11.75

Statistically significant differences ($p<0.005$, one-way ANOVA and Student's T-test with Bonferroni correction) versus vehicle samples were highlighted in green (C= CC214-2 responsive xenografts; R= CC214-2 resistant xenografts; D= dasatinib; U= U0126; C+D= CC214-2 + dasatinib; C+U= CC214-2 + U0126; DR= Drug Removed). Values represent the average of all the data points extracted from the xenograft samples in each treatment group.

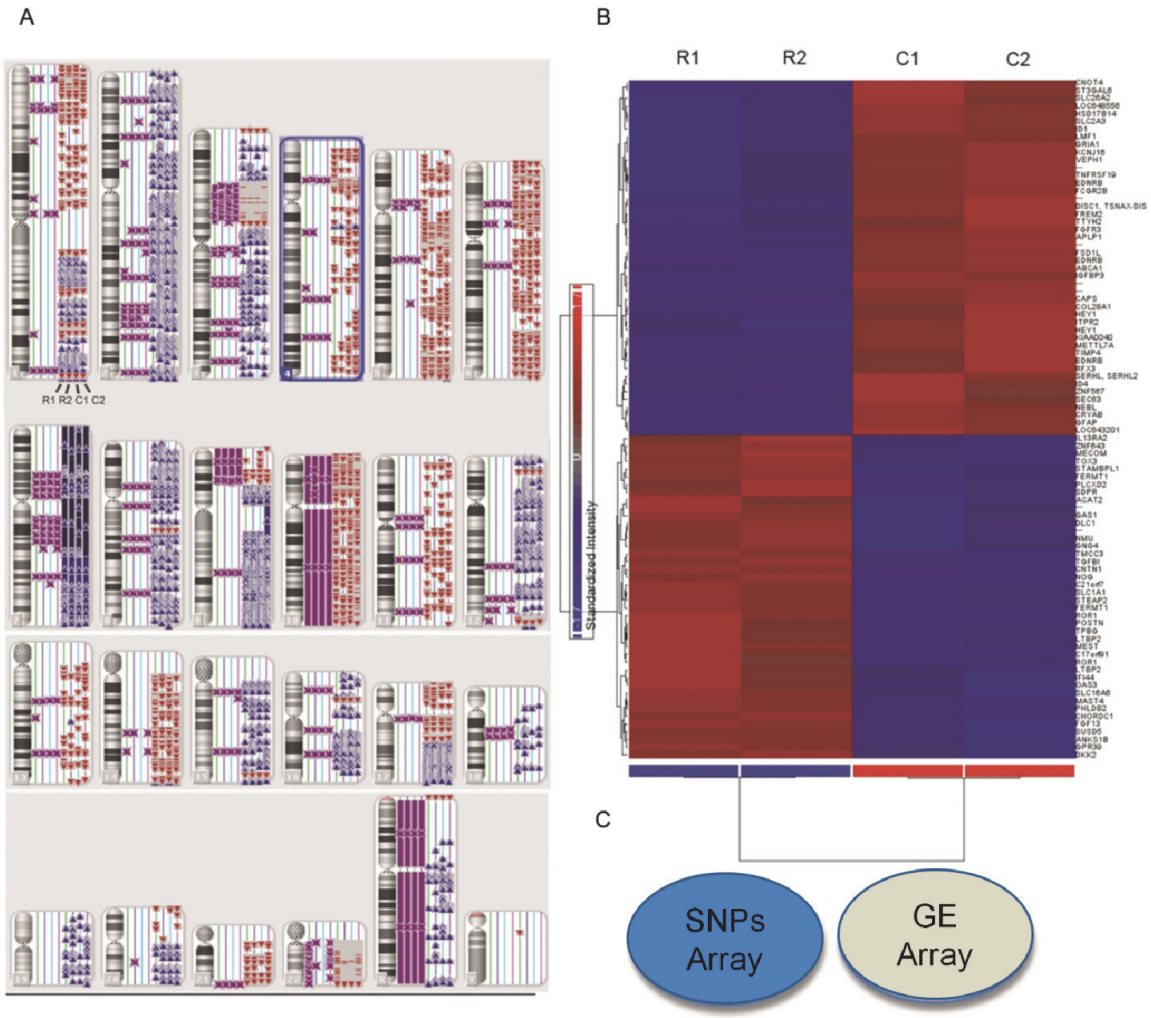

Figure S2, related to Figure 2. Karyotype Copy Number Variations (CNVs) identified by Single Nucleotide Polymorphism (SNPs) analysis and Gene Expression (GE) profiles. (**A**) Two control, C1-2 (right two lanes), and two CC214-2 resistant samples, R1-2 (left two lanes), were analyzed by Affymetrix SNP array 6.0, using a filter of 200 kb and 50 markers for the copy number variation analysis. Although all of these samples show a very unstable genome, only 18 CNVs discriminated the resistant samples from the control samples (Table S4). Gains and losses are shown respectively in blue and red colors; magenta crosses along the CNVs indicate DNA Loss Of Heterozygosity (LOH). (**B**) Affymetrix U133plus2.0 arrays were used to perform GE analysis on matched resistant and control samples identifying a group of 88 discriminating genes (Table S5). The list of genes is mentioned in the right y-axis, the sample's names are listed in the above x-axis. Gains and losses are shown respectively in red and blue colors. (**C**) SNPs and GE analyses did not show any overlapping calls.

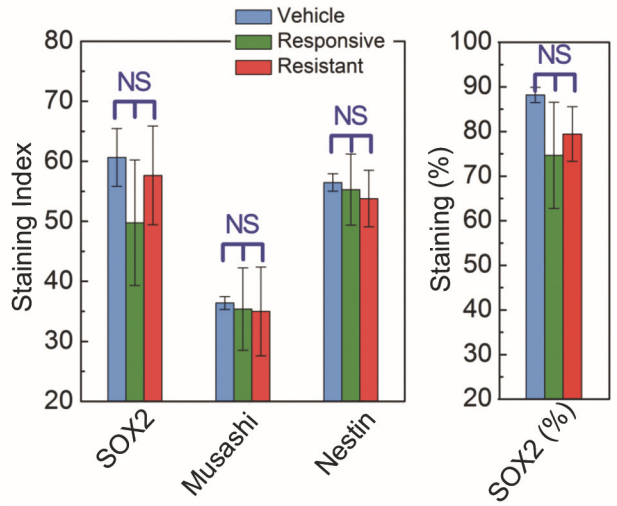

Figure S3, related to Figure 2. Populations of stem cell markers over the course of CC214-2 therapy. The intensities among different groups were compared via one-way ANOVA. No statistically significant difference is identified (data are shown as mean +/- SD, NS: not significant).

Table S2, related to Figure 2, Shared LOH of responsive and resistant samples compared to control identified by Whole Exome Sequencing (WES).

Mutation	Chrom.	Type
RGPD8, G1570R	chr2	hom
OR52L1, C140R	chr11	hom
KRT40, T37A	chr17	hom
CYP2A6, F392Y	chr19	hom
AURKA, I57V	chr20	hom
NUAK2, P441P	chr1	hom
PREX2, K33K	chr8	hom
KCNJ11, A190A	chr11	hom

Non-synonymous mutations are labeled in yellow and synonymous mutations are labeled in blue.

Table S3, related to Figure 2, Somatic mutations and small INDELs in control, responsive, and resistant GBM39 xenograft samples identified by Whole Exome Sequencing (WES). (See Excel file attached)

Table S4, related to Figure 2, Karyotype Copy Number Variations (CNVs) identified by Single Nucleotide Polymorphism (SNPs) analysis. (See Excel file attached; samples 1, 5: control samples; samples 3, 4: resistant samples)

Table S5, related to Figure 2, Differential Gene Expression (GE) identified by Affymetrix U133 plus 2.0 arrays. (See Excel file attached; treated samples indicate CC214-2 resistant GBM39 xenografts)

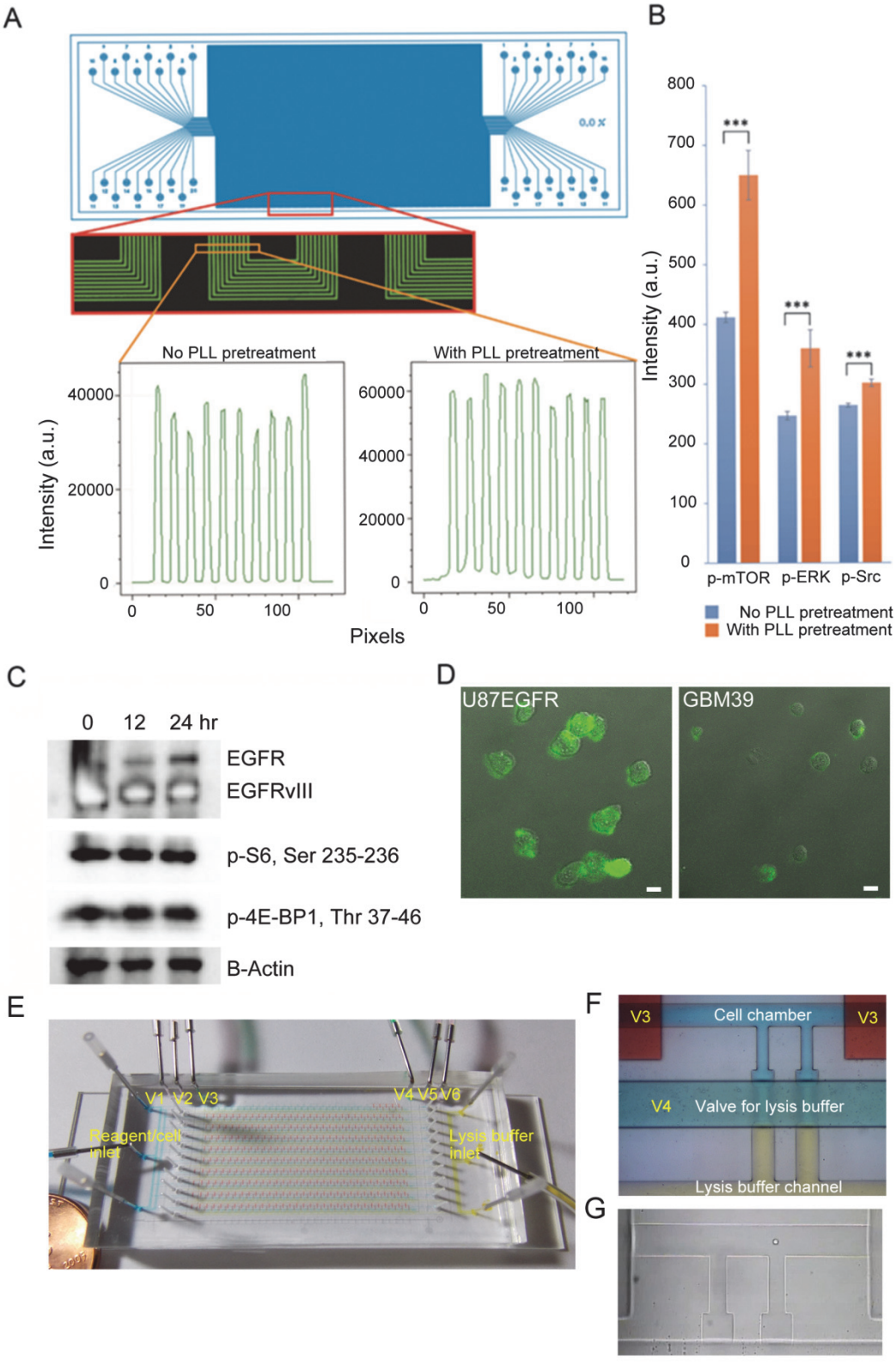

Figure S4, related to Figure 3. Preparation of DNA barcode microarray for single cell proteomic test. (A) Design and validation of the DNA flow patterning device. The PLL pretreatment improves the ssDNA loading about

2 fold as reflected in the fluorescence intensity from Cy3-linked complementary ssDNA hybridization, and therefore increases the sensitivity of the protein detection. **(B)** Representative of measured protein levels of single cells from a GBM39 mouse xenograft sample (data are shown as mean +/- SD). $EGFR^+$ cells were pre-sorted by magnetic beads and analyzed by SCBCs with or without PLL pretreated slide respectively. Three representative phosphoproteins were detected by sandwich fluorescence immunoassays with an Alexa-Fluor 647 readout. Higher DNA loading in the PLL pretreated device enabled conversion of the ssDNA microarray to a much denser antibody microarray by flowing complementary ssDNA-antibody conjugates, and thus allowed to detect proteins with higher signal intensities and sensitivity. Student's T-test was used to evaluate the statistical significance (***$p<0.001$). **(C)** Western blot results for the cells that were sorted, plated and harvested at three different time points: 0, 12, 24 hr. The levels of key functional proteins do not change over time, validating the cell plating step for the test. **(D)** EGFR expression level of sorted U87/EGFR cells and GBM39 cells. After sorting, cells were stained with PE-conjugated rat anti-human EGFR antibodies. The image showed that GBM39 cells are smaller in size but are more heterogeneous in terms of EGFR expression on the cell membrane (scale bar: 10 μm). **(E)** Picture of SCBC. V1-V6 denote valve 1 to valve 6. **(F)** Picture of one chamber unit: valves for chamber formation (red), valve for lysis buffer control (green), cell chamber compartment (blue), and lysis buffer (yellow) reservoir are delineated by food dyes. **(G)** Optical image of a single cell chamber.

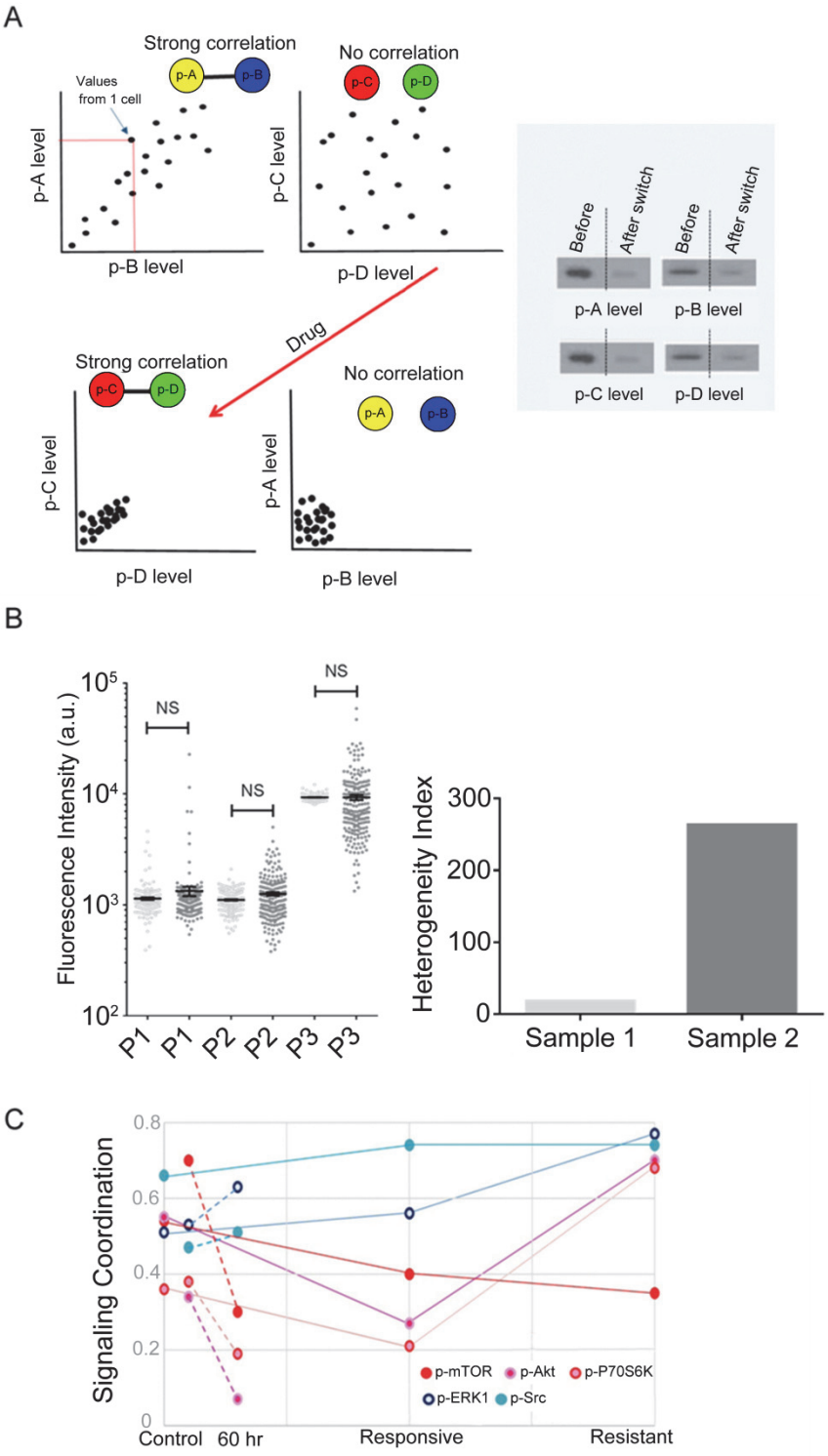

Figure S5, related to Figure 4. Single cell assays resolve protein signaling coordination. (A) The hypothetical experiment involves measuring 4 phosphoproteins from single cancer cells. The top scatter plots show that the levels of p-A and p-B are strongly correlated, while the levels of p-C and p-D are uncorrelated, consistent with a strong interaction between p-A and p-B. Drugging the cells represses the levels of all 4 proteins, but increases the correlations between p-C and p-D, indicating that a signaling network containing p-C and p-D was activated in

response to the drug. Traditional immunoblotting assays miss this drug-induced activation. (**B**) Illustration of the heterogeneity index for a hypothetical single cell test on two samples with 3 proteins in panel. The two hypothetical samples have statistically undistinguishable average protein levels but dramatically different protein distributions, leading to a clear difference in the heterogeneity index. Statistical uniqueness is evaluated by two-tail Mann-Whitney test for pairwise comparison (*$p<0.05$; **$p<0.005$; ***$p<0.0005$; NS: not significant). **(C)** Complete signaling coordination analysis for GBM39 (solid lines: in vivo; dash lines: in vitro).

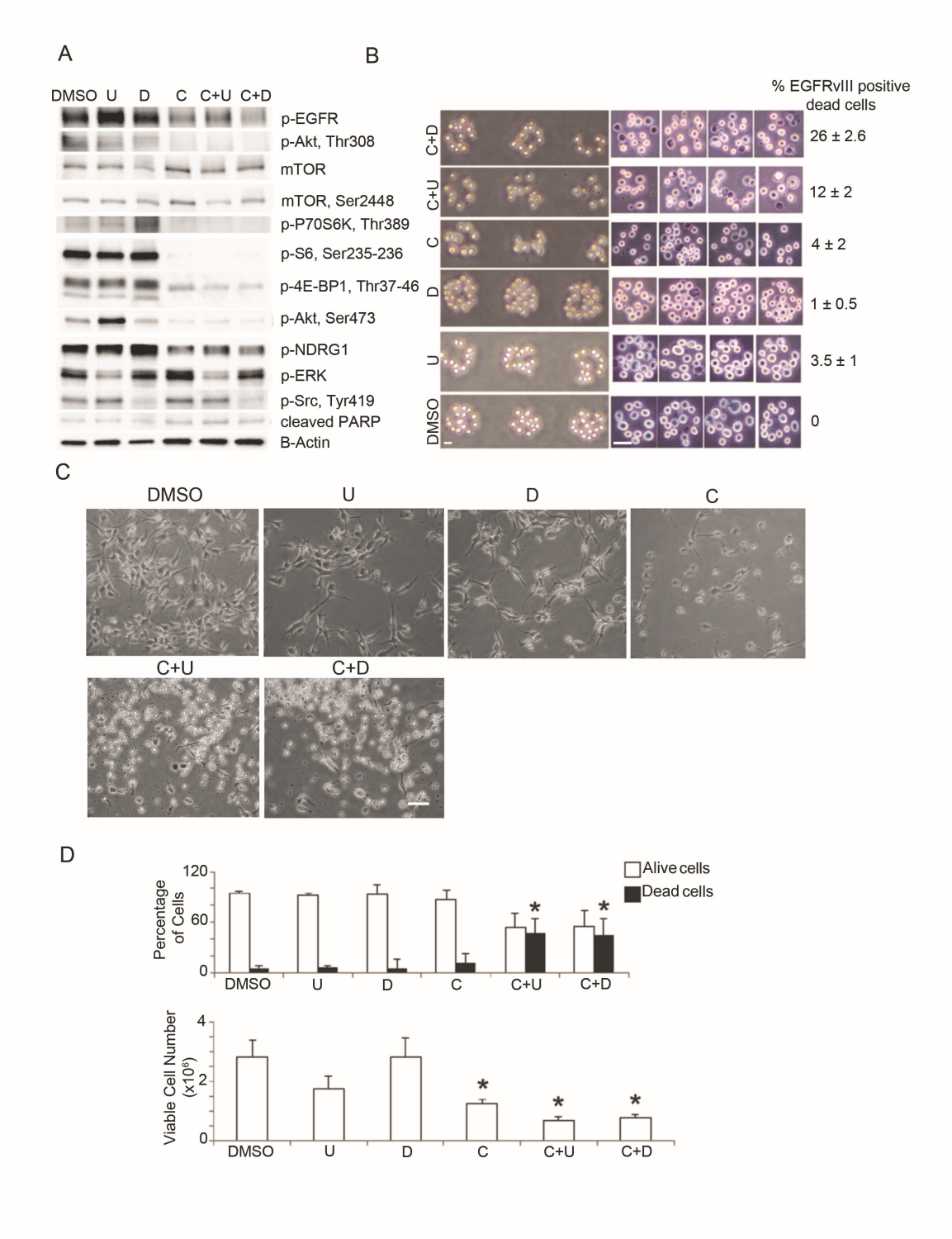

Figure S6, related to Figure 5. In vitro GBM39 combinatory treatment with CC214-1, U0126 and dasatinib. **(A)** Biochemical analysis of the drug targets down-regulation upon single or combinatory treatments. All of the drugs successfully hit their targets. (U: 5 μM U0126, D: 100 nM dasatinib, U+C: U0126 + 2 μM CC214-1, D+C: dasatinib + CC214-1; 24 hr treatment). **(B)** DEAL sorting of GBM39 EGFR+ cells after single or combinatory treatments, followed by trypan blue assay. Cells were treated with CC214-1, U0126 and dasatinib for 4 days at the

concentration specified in (A). The percentages of dead cells are listed on the right side of the images. Cell death percentages resulted significantly different from DMSO in the combinatory treatments. Data are represented at mean +/- SD of three independent experiments. **(C)** In vitro GBM39 proliferation assay after combinatory treatments with CC214-1, U0126 and dasatinib (3-day treatment). Representative images of the GBM39 cells under treatment are shown. **(D)** Bar graphs of the percentage of viable and dead cells and the total viable cell number for the treated cells depicted in (A); *$p<0.05$ relative to treated versus DMSO samples (one-way ANOVA and Student's T-test with Bonferroni correction. Data are representative of three independent experiments). Scale bars: 100 μm. Error bars: +/- SD.

Table S6, related to Figure 6. Explanatory and dependent matrices used for PLS modeling.

	Explanatory Metrics										Dependent Metrics	
	Tunel	Ki-67	p-Src	p-ERK	HIF-1α	p-P70S6K	p-S6	p-4E-BP1	p-Akt	p-NDRG1	TGR at Sacrifice (%)	Cell Cycle Measure (τ) (Days)
V1	0.17	38.95	14.93	17.52	14.23	12.24	22.05	13.49	11.07	19.57	19	6.61
C	1.46	25.96	19.98	11.49	12.71	8.78	15.90	9.47	7.51	11.94	7.7	8.3
D	0.22	40.37	15.46	17.24	13.89	11.24	18.98	13.56	10.67	23.15	8.6	6.56
U	0.18	41.41	13.00	7.68	14.76	10.71	17.19	14.21	9.76	22.91	16	6.02
U+D	0.29	40.32	8.10	6.81	10.89	10.55	17.19	12.93	11.30	22.65	12.7	7.01
C+D	1.75	29.30	9.26	13.75	13.08	8.68	11.76	8.36	5.82	5.06	7.1	17.98
C+U	1.23	27.53	16.77	11.11	13.09	9.03	10.56	9.09	5.88	4.72	5.28	15.99
C-R	0.17	40.20	19.32	25.89	16.52	10.29	23.19	20.22	16.90	26.47	18.5	5.84
C+D DR	0.07	49.91	18.61	15.05	10.59	12.62	18.55	17.60	10.20	21.37	33	2.73
C+U DR	0.10	52.60	14.57	15.35	14.52	10.93	19.59	12.52	9.69	21.70	15.7	5.45
V2	0.13	43.44	14.82	17.13	13.40	11.50	18.34	12.86	11.02	21.29	16.59	6.58

The explanatory matrix is composed of numerical IHC data for samples treated under different drug combinations, including V1 for vehicle, C for CC214-2 treated, D for dasatinib treated, U for U0126 treated, U+D for combinatory treatment of U0126 and dasatinib, C+D for CC214-2 and dasatinib, C+U for CC214-2 and U0126, C-R for resistant stage of CC214-2 treated sample, C+D DR for C+D treated samples after drug removal, C+U DR for C+U treated samples after drug removal and V2 for the control sample in the first CC214-2 only in vivo experiment. The values of TGR at sacrifice and cell cycle measure are directly extracted from the corresponding growth curves under different drug treatments. The orange part of the table represents the calibration phase of the model and blue part represents the prediction phase.

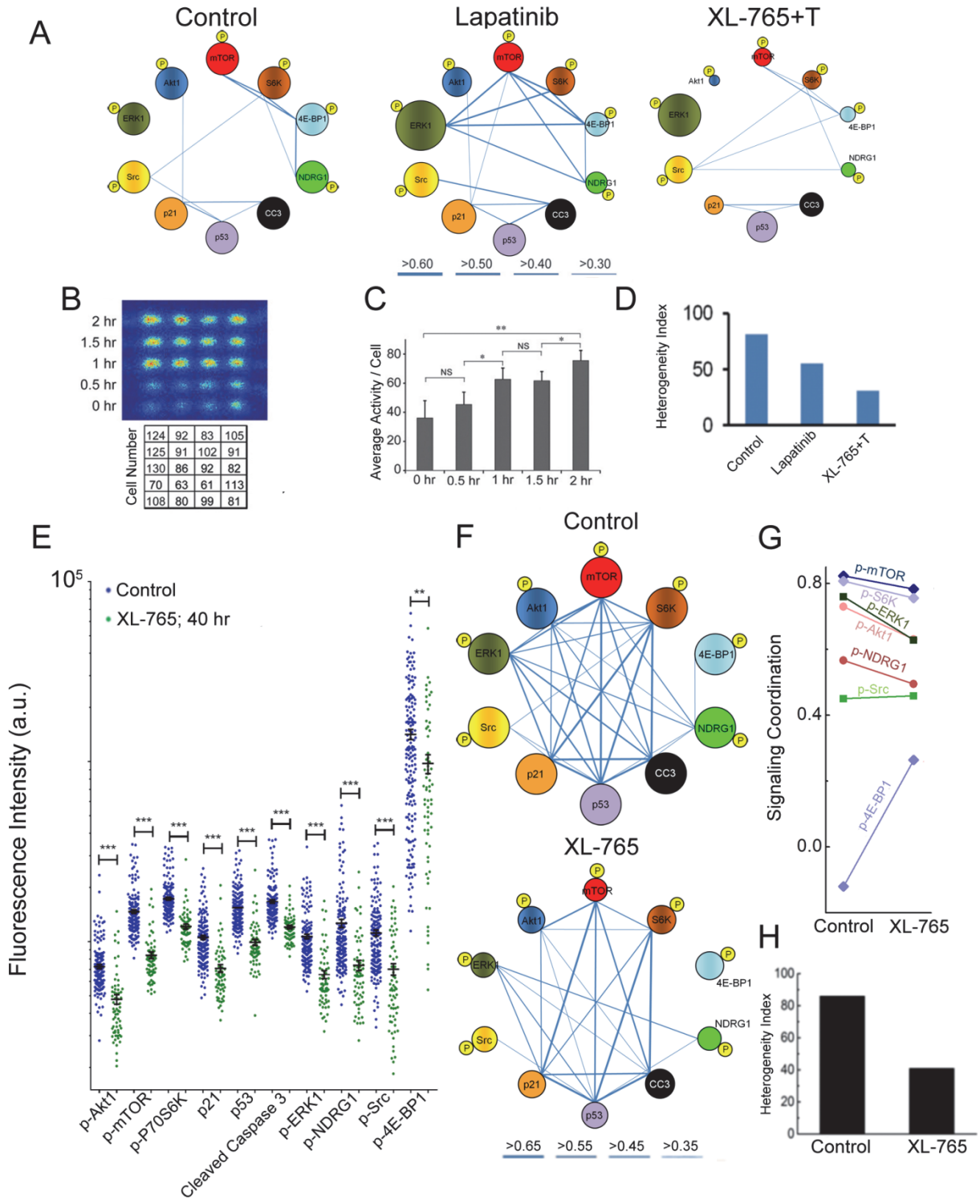

Figure S7, related to Figure 7. Single-cell analysis and in vitro validations on the pcGBM2 cell line and a freshly resected recurrent GBM patient sample. (A) Protein-protein correlation networks for control, lapatinib and XL-765+T treated samples, extracted from single-cell data. Averaged protein levels are reflected in the sphere diameters, while correlation strengths are reflected in the thickness of the edges (see key). **(B)** Glucose uptake

kinetics for lapatinib treated cells are profiled by a microchip based radioassay using ^{18}F-FDG as a probe. (**C**) Quantification of glucose uptake kinetics indicates an elevated glucose consumption of tumor cells within the first 2 hr under lapatinib treatment (data are shown as mean +/- SD). Statistical uniqueness is evaluated by Student's T-test for pairwise comparison (*p<0.05; **p<0.005; NS: not significant). **(D)** Heterogeneity indices of the cancer cells at control, lapatinib and XL-765+T treated stages. **(E)** SCBC analysis of a recurrent GBM patient sample. One-dimensional scatter plots of single-cell protein measurements, for a panel of 10 proteins. Following resection, the cells were either untreated, or treated with the mTOR inhibitor XL-765 for 40 hr. All protein levels are repressed following treatment. The averaged fluorescence intensity with standard error of the mean (SEM) is overlaid for each protein (black horizontal bars). Statistical uniqueness is evaluated by two-tail Mann-Whitney test for pairwise comparison (*p<0.05; **p<0.005; ***p<0.0005; NS: not significant). **(F)** Signaling network correlations for control and XL-765 treated tumor cells. The sphere diameters represent protein abundances, while the edges represent protein-protein correlations. The strength of the correlation is related to edge thickness, as given in the key. **(G)** Correlation between key functional proteins and the PC1 for control and XL-765 treated samples. **(H)** Heterogeneity indices of the tumor cells with and without XL-765 treatment.

Supplemental Experimental Procedure

Cell lines, primary cells and reagents. GBM39 primary neurospheres were previously described (Nathanson et al., 2014) and authenticated by luciferase reporter expression before the beginning of the in vivo experiments. GBM39 cells were tested for pathogens, including mycoplasma, by IDEXX RADIL and all tests results were negative. GBM39 cells were cultured in NeuroCult (StemCell Technologies) supplemented with Heparin (1 μg/mL; SIGMA), Epidermal Growth Factor (EGF, 20 ng/mL; SIGMA) and Fibroblast Growth Factor (FGF, 20 ng/mL; SIGMA) and 100 U/mL penicillin and streptomycin (Gibco) in a humidified 5% CO_2 (vol/vol) incubator, at 37°C. The pcGBM2 cell line derived from a 15-year old male patient bearing $EGFRvIII^+$ GBM tumor, was provided by Dr. Michelle Monje (Stanford University) as a gift upon informed consent following the Stanford University Ethical Committee regulations. The cells were cultured in tumor sphere media (TSM) consisting of Dulbecco's Modified Eagle Media Nutrient Mix F-12 (DMEM/F-12, Invitrogen), Glutamax-I (Invitrogen), Neurobasal (Invitrogen), B27 (Invitrogen), human-bFGF (20 ng/mL) (Shenandoah Biotech), human-EGF (20 ng/mL) (Shenandoah Biotech), human-PDGF-AA (Shenandoah Biotech), human-PDGF-BB (Shenandoah Biotech) and heparin (10 ng/mL). The recurrent GBM patient sample was collected from a freshly resected, recurrent GBM tumor from a 73-year old male patient upon informed consent following the UCLA Ethical Committee regulations. The tumor has been characterized as IDH1/2 negative, PTEN null and no EGFR amplification. The resected tumor was blood cell depleted and dissociated into single cell suspension immediately after collection from the operating room. CC214-1 and CC214-2 were provided by Celgene Corporation (San Diego, U.S.A.) (Mortensen et al., 2013). Lapatinib ditosylate (GW-572016), trametinib (GSK1120212) and XL-765 (SAR245409) were purchased from Selleckchem. The antibodies used for SCBC tests as well as for the immunoblotting and IHC were listed below.

Reagents Used. The upper part of the table provides the sequences of the oligonucleotides used in the protein immunoassays. All oligonucleotides were synthesized by Integrated DNA Technology (IDT) and purified via high performance liquid chromatography (HPLC). The DNA coding oligomers were pre-tested for orthogonality to ensure that cross-hybridization between non-complementary oligomer strands was negligible (<1% in photon counts). Below the oligonucleotides is a list of the antibodies and standard proteins used for the SCBC multiplex protein assay as well as for the immunoblotting and the IHC.

Name	DNA Sequence	Melting Point
B	5'-AAA AAA AAA AAA AGC CTC ATT GAA TCA TGC CTA -3'	57.4
B'	5' NH3AAA AAA AAA ATA GGC ATG ATT CAA TGA GGC -3'	55.9
C	5'- AAA AAA AAA AAA AGC ACT CGT CTA CTA TCG CTA -3'	57.6
C'	5' NH3-AAA AAA AAA ATA GCG ATA GTA GAC GAG TGC -3'	56.2
D	5'-AAA AAA AAA AAA AAT GGT CGA GAT GTC AGA GTA -3'	56.5
D'	5' NH3-AAA AAA AAA ATA CTC TGA CAT CTC GAC CAT -3'	55.7
E	5'-AAA AAA AAA AAA AAT GTG AAG TGG CAG TAT CTA -3'	55.7
E'	5' NH3-AAA AAA AAA ATA GAT ACT GCC ACT TCA CAT -3'	54.7
F	5'-AAA AAA AAA AAA AAT CAG GTA AGG TTC ACG GTA -3'	56.9
F'	5' NH3-AAA AAA AAA ATA CCG TGA ACC TTA CCT GAT -3'	56.1

G	5'-AAA AAA AAA AGA GTA GCC TTC CCG AGC ATT-3'	59.3
G'	5' NH3-AAA AAA AAA AAA TGC TCG GGA AGG CTA CTC-3'	58.6
H	5'-AAA AAA AAA AAT TGA CCA AAC TGC GGT GCG-3'	59.9
H'	5' NH3-AAA AAA AAA ACG CAC CGC AGT TTG GTC AAT-3'	60.8
I	5'-AAA AAA AAA ATG CCC TAT TGT TGC GTC GGA-3’	60.1
I’	5' NH3-AAA AAA AAA ATC CGA CGC AAC AAT AGG GCA-3’	60.1
K	5'-AAA AAA AAA ATA ATC TAA TTC TGG TCG CGG-3'	55.4
K'	5' NH3-AAA AAA AAA ACC GCG ACC AGA ATT AGA TTA-3'	56.3
L	5'-AAA AAA AAA AGT GAT TAA GTC TGC TTC GGC-3'	57.2
L'	5' NH3-AAA AAA AAA AGC CGA AGC AGA CTT AAT CAC-3'	57.2
M	5'-AAA AAA AAA AGT CGA GGA TTC TGA ACC TGT-3'	57.6
M'	5' Cy3-AAA AAA AAA AAC AGG TTC AGA ATC CTC GAC-3'	56.9
DNA Label	**Antibody for Conjugation in SCBC**	**Source**
B’	Human/Mouse p-Akt1 (S473) DuoSet® IC ELISA kit	R&D DYC2289B
C’	Human p-TOR (S2448) DuoSet® IC ELISA kit	R&D DYC1665
D’	Human p-p70 S6 Kinase (T389) DuoSet® IC ELISA kit	R&D DYC896
E’	Human Total p21/CIP1/CDKN1A DuoSet® IC ELISA kit	R&D DYC1047
F’	Human Total p53 DuoSet® IC ELISA kit	R&D DYC1043
G’	Human/Mouse Cleaved Caspase-3 (Asp175) DuoSet® IC ELISA kit	R&D DYC835
H’	Human/Mouse/Rat p-ERK1 (T202/Y204) DuoSet® IC ELISA kit	R&D DYC1825
I’	Human NDRG1	Capture - R&D AF5209
	p-NDRG1 (Thr346)	Detection - Cell Signaling 7497
K’	Human p-Src (Y419) DuoSet® IC ELISA kit	R&D DYC2685
L’	Human total HIF-1α DuoSet® IC ELISA kit	R&D DYC1935
L’	Human 4E-BP1	Capture - R&D AF3227

	p-4E-BP1 (Thr37-46)	Detection - Cell Signaling 5123
Catalog #	**Antibody for Immunoblotting and IHC**	**Source**
4060	p-Akt Ser473 (D9E)	Cell Signaling
9275	p-Akt Thr308	Cell Signaling
4857	p-S6 Ser235-236 (91B2)	Cell Signaling
9205	p-P70S6K Thr389	Cell Signaling
2855	p-4E-BP1 Thr37-46 (236B4)	Cell Signaling
4370	p-ERK Thr202-204 (D13.14.4E)	Cell Signaling
2971	p-mTOR Ser2448	Cell Signaling
2976	p-mTOR Ser2448 (49F9)	Cell Signaling
2972	mTOR	Cell Signaling
2101	p-Src Tyr416	Cell Signaling
3217	p-NDRG1 Thr346	Cell Signaling
5482	p-NDRG1 Thr346 (D98G11)	Cell Signaling
2280	raptor (24C12)	Cell Signaling
06-847	EGFR	Millipore
36-9700	p-EGFR Tyr1086	Invitrogen
2997	p-PRAS40 Thr246 (C77D7)	Cell Signaling
441100G	p-PRAS40 Thr246	Invitrogen
9541	cleaved PARP Asp214	Cell Signaling
ABM-2052	PTEN (6H2.1)	Cascade Bioscience
VP-RM04	Ki-67 (SP6)	Vectorlabs
SMC-184D	HIF-1α	StressMarq
16314-015	TUNEL	Invitrogen
NB-600-501	Actin (AC15)	Novus Biologicals
D270-3	Musashi	MBL
sc-23927	Nestin	Santa Cruz Biotechnology
MAB4343	SOX-2	Millipore

In vivo experiment. GBM39 flank xenografts (Figures 1, 2 and 5) were obtained in full compliance with the UCLA-Division of Laboratory Animal Medicine (DLAM) regulation and with the UCSD-Institution of Animal Care and Use Committee (IACUC) regulations. GBM39 cells were resuspended in PBS (Cellgro) plus Matrigel (BD Biosciences), 1:1 solution (vol/vol), at 1×10^7 cells/ml density. One million of GBM39 cells were injected in the flank of each 4 weeks old female athymic mouse. Tumor sizes were measured using automated caliper. For the drug treatments, CC214-2 was administered by oral gavage, 100 mg/kg, once every two days, in a suspension containing 0.5% carboxymethylcellulose (Sigma), 0.25% Teewn-80 (Sigma) in nanopure water. Dasatinib (Selleckchem) was

administered by oral gavage, 30 mg/kg, once every two days, dissolved in the CC214-2 suspension. U0126 (Selleckchem) was administered by intra-peritoneal injection, 25 μmol/kg, once every two days, in a suspension containing 40% DMSO (vol/vol, Fisher) in PBS (Cellgro). The injection of 1 mL saline 0.9% NaCl (Baxter) was used if signs of weight loss were registered. Mice were euthanized when tumors reached 15 mm diameter. To determine the number of animals requested, we carried out power calculations using STATA software (version 8), performed the Monte Carlo simulation command (simpower) and determined the sample size to detect a significant difference in our tumor size comparison study. To ensure statistical significance of drug effects, we used a sufficient, but not excessive, sample size: for vehicle treated controls, CC214-2 responsive and CC214-2 resistant mice n = 11, 7, 7 respectively for each group; for dasatinib, U0126, either alone or in combination, and for the combinatory treatments with CC214-2, n = 4 for each group.

Mice were kept un-labeled until the beginning of the treatments allowing to allocate them randomly to each treatment group. Caliper measurements were assessed in blind by multiple investigators. One-way ANOVA and Student's T-test with Bonferroni corrections were used to assess statistical significance (GraphPad Prism). The variation between groups was similar and expressed as standard deviation.

MicroPET/CT imaging. Four mice for each group were anesthetized with isoflurane (2% in 100% oxygen), warmed and injected with 20 μCi [F^{18}]-FDG. After an uptake period of 60 min, mice were placed in a dedicated imaging chamber designed for use for the CT and both PET systems. Data were acquired using an Inveon scanner (Siemens Preclinical Solutions), a Genisys4 (Sofie Biosciences, Culver City, CA) and a MicroCAT II CT (microCAT; Imtek Inc.) instrument. Acquisition of PET images was performed for 10 min on each scanner followed by 8 min CT acquisition (Fueger et al., 2006).

PET and CT Images were analyzed using OsiriX Imaging Software (version 3.8; OsiriX). MicroCT and PET images were reviewed blinded to detect tumor burden. Consecutive 2-dimensional regions of interest (ROI) were drawn on tumor on coronal and axial to detect the maximum FDG uptake. These regions encompassed the entire metabolically active tumor. Display of representative images was done according the shown color scale proportional to tissue concentration, with red being the highest and lower values in yellow, green, and blue (Figures 1B and S1A). One-way ANOVA and Student's T-test with Bonferroni correction were used to assess statistical significance (GraphPad Prism).

IHC. Paraffin embedded GBM39 xenografts blocks were sectioned at the UCLA Pathology Histology and Tissue Core Facility and at the UCSD Histology and IHC core followed by IHC stains (antibodies listed in Table above) performed as described in Mellinghoff et al (Mellinghoff et al., 2005). Three images at 40x magnification per IHC slide were captured using DP 26 camera mounted on an Olympus BX43 microscope. Quantitative single cell analysis of the IHC stained slides was performed with Microsuite Five software (Olympus). In the IHC quantification, the following number of xenografts was considered for each group: n= 7 for controls, n= 6 for CC214-2 responsive group, n= 5 for CC214-2 resistant group, n= 4 for dasatinib group, n= 4 for U0126 group, n= 4 for U0126 plus dasatinib group, n= 2 for each combination with CC214-2, n= 2 for each drug removed group. One-way ANOVA and Student's T-test with Bonferroni correction were used to assess statistical significance (GraphPad Prism).

Immunoblotting. Western blot was done loading 10 μg of protein lysates. Lysates were collected in RIPA buffer (Boston BioProducts) with addiction of protease plus phosphatase inhibitor cocktail, 10μL/mL each (Thermo Scientific). Gradient 4-15% pre-casted gels were used for the electrophoretic protein separation in mono-dimension (Bio-Rad). Proteins were transferred on nitrocellulose membranes using Trans-blot Turbo Transfer system (Bio-Rad). Blots were then blocked in Tris-buffered saline, 0.1% Tween20 (vol/vol) and 5% BSA (Fischer Scientific, vol/vol) for 1 hr. The primary antibodies were incubated over-night, at 4ºC. After washing, the membranes were incubated with secondary HRP conjugated antibodies for 1 hr at room temperature. West Femto Trial kit (Thermo Scientific) was used to develop the immunoreactivities.

Whole Exome Sequencing (WES) analysis. The molecular profile of GBM39 xenografts, including copy number alterations, mutations in common oncogenes, and transcriptional signature was previously characterized (Hodgson et al., 2009 – data deposited into GEO - GSE14806) and was further characterized as part of the TCGA GBM project (Verhaak et al., 2010). GBM39 contains *EGFR* amplification and *EGFRvIII* mutation, among other lesions, and has a transcriptional profile of the "classical" GBM subtype (Verhaak et al., 2010). We further analyzed with next generation sequencing the GBM39 PDXs. A range of 6-14 μg of gDNAs were extracted from the GBM39 xenografts at control, responsive and resistant stages using Qiagen QIAamp DNA Mini kit. Whole-exome DNA was

captured from total genomic DNA using the SeqCap EZ System from NimbleGen according to the manufacturer's instructions. Briefly, genomic DNA was sheared, size selected to roughly 200-250 base pairs, and the ends were repaired and ligated to specific adapters and multiplexing indexes. Fragments were then incubated with SeqCap biotinylated DNA baits followed by the LM-PCR, and the RNA-DNA hybrids were purified using streptavidin-coated magnetic beads. The RNA baits were then digested to release the targeted DNA fragments, followed by a brief amplification of 15 or less PCR cycles. The libraries were then sequenced on the NextSeq 500 platform from Illumina, using 100-bp pair-ended reads and an average coverage ≥ 100X.

The sequence data were aligned to the GRCh37 human reference genome using BWA v0.7.7-r411. PCR duplicates were marked using MarkDuplicates program in Picard-tools-1.115 tool set. GATK v3.2-2 was used for INDEL (insertions and deletions) realignment and base quality recalibration. Exome coverage was calculated using the bedtools. Samtools was used to call the SNVs (single nucleotide variants) and small INDELs. Somatic mutations calling was performed using Varscan 2.0 (min. coverage 10, min. var. freq. 0.04, somatic p value 0.05). Varscan2 calculates the significance of allele frequency difference between treatment and control by Fisher's Exact Test. If the difference is significant (p-value < threshold), somatic SNV or LOH will be called. The NextSeq 500 can reliably detect subclonal variants if the percentage of subclonal population is ≥ 5% as heterozygous variant or ≤ 2.5% as homozygous variant. All variants were annotated using the Annovar program. SNPs identified in the 1000 Genomes project or in dbSNP138 database were removed. Synonymous changes were identified and filtered from the variant list using SIFT software. PROVEAN/SIFT programs were used to analyze the SNVs function of relevant proteins. WES analysis data have been deposited in SRA and the accession code is SRP062496.

Single Nucleotide Polymorphism (SNPs) and Gene Expression (GE) analyses. We further interrogated the genome and the transcriptome of two matched vehicle and resistant samples respectively using Single Nucleotide Polymorphism (SNPs) and Gene Expression (GE) arrays analyses. Two controls and two CC214-2 resistant PDXs were used for the DNA extractions, using the Qiagen QIAamp DNA Mini kit protocol. Five hundred ng of DNA from control and resistant samples were analyzed by Affymetrix SNP 6.0 array (200 kb filter, 50 markers) at the Clinical Microarray Core, University of California Los Angeles. SNPs analysis data have been deposited to Gene Expression Omnibus (GEO). The accession code is GSE53042. Gene expression analysis was performed at the same core by Affymetrix U133plus2.0 array using 200 ng of RNA extracted from the same two controls and two CC214-2 resistant xenografts used in the SNPs screening (Qiagen micro RNA extraction kit). Those genes from the resistant samples with expression fold changes above 1.5 fold relative to the vehicle treated samples were considered statistically significant in the analysis. A group of 88 genes was identified using these parameters. Microarray gene expression analysis data have been deposited into GEO. The accession code is GSE63387.

Procedure for preparing single cell suspension from solid tumor. Freshly resected xenografts were finely cut in sterile conditions and digested for 3 hr at 37°C, under constant rotation (200 rpm), in a solution containing 1.5% BSA (g/mL, Gemini), 0.3% collagenase type 2 (g/mL, Worthington), 0.3% collagenase type 4 (g/mL, Worthington) and 10 μg/mL DNAse I enzyme (Sigma). Single cell suspensions were then filtered with a 40 μm cell strainer and pellets were treated for 2 min with 3 mL ACK buffer (Lonza). Solutions were neutralized with DMEM medium (Gibco) and cell viability assessed by trypan blue exclusion. Frozen stocks were made re-suspending cell pellets in Bambanker (Wako) and storing cryovials at – 80°C.

Synthesis of DNA-1° antibody conjugates. As-received antibodies were desalted, buffer exchanged to pH 7.4 PBS and concentrated to 0.5 mg/mL using Zeba protein desalting spin columns (Pierce). Succinimidyl 4-hydrazinonicotinate acetone hydrazine (SANH, Solulink) in *N*,*N*-dimethylformamide (DMF) was added to the antibodies at variable molar excess (300:1). Separately, succinimidyl 4-formylbenzoate (SFB, Solulink) in DMF was added at a 16-fold molar excess to 5'aminated 30 mer oligomers in PBS. After incubation for 4 hr at room temperature, excessive SANH and SFB were removed by buffer exchange of both samples to pH 6.0 citrate buffer using protein desalting spin columns. A 30-fold excess of derivative DNA was then combined with the antibody and allowed to react 2 hr at room temperature followed by overnight incubation at 4°C. Non-coupled DNAs were removed by FPLC with Pharmacia Superdex 200 gel filtration column (GE) at 0.5 mL/min isocratic flow of PBS. The conjugates were then concentrated to 0.5 mg/mL by Amicon Ultra-4 Centrifugal Filter Unit with Ultracel-10 membrane (Millipore 10kDa) and stored at 4°C. The conjugation yield was determined by protein BCA assay with Nanodrop 2000C (Thermo Scientific).

Microchip Fabrication. The SCBCs were assembled from a DNA barcode microarray glass slide and a PDMS slab containing a microfluidic circuit. The DNA barcode array was created with microchannel-guided flow patterning.

The PDMS chips for DNA patterning were fabricated by soft lithography. The master mold for the PDMS chips was prepared by SU8 2015 negative photoresist. The mold has long meandering channel lines with 20 μm and 30 μm in width and height, respectively. The mixture of Sylgard PDMS (Corning) prepolymer and curing agent in 10:1 ratio (w/w) was poured onto the mold, degassed in a homemade vacuum chamber and cured at 80°C for 1 hr. The cured PDMS slab was released from the mold, inlet/outlet holes punched, and bonded onto a poly-L-lysine (PLL) coated glass slide (Thermo scientific) to form enclosed channels. The number of microfluidic channels determines the size of the barcode array and 10 parallel microchannels were used in this study. The PDMS microfluidic chip for the cell experiment was fabricated using a two-layer soft lithography approach. The control layer was molded from a SU8 2025 negative photoresist (~ 40 μm in thickness) silicon master using a mixture of GE RTV 615 PDMS prepolymer part A and part B (10:1). The flow layer was fabricated by spin-casting the pre-polymer of GE RTV 615 PDMS part A and part B (20:1) onto a SPR 220 positive photoresist master at ~2000 rpm for 1 min. The SPR 220 mold was ~ 12 μm in height after rounding via thermal treatment. The PDMS part for control layer was then carefully aligned and placed onto the flow layer, which was still situated on its silicon master mold. An additional 60 min thermal treatment at 80^{o}C was performed to enable bonding. Afterward, this two-layer PDMS chip was cut off and access holes drilled. Finally, the microfluidic-containing PDMS slab was thermally bonded onto the barcode-patterned glass slide to yield a fully assembled microchip.

DNA barcode chip patterning and validation. DNA barcode patterns are prepared as described elsewhere (Shin et al., 2010) with slight modification. Since the primary cells are smaller in size and have a higher dynamic range in terms of oncogenic signaling compared to the genetic modified cell lines (Figure S4D), an antibody microarray with better sensitivity is critical, which in turn requires higher DNA loading for the patterning. To increase the loading, an additional PLL coating step was included. After bonding of the PDMS device to the PLL slide, 0.1% PLL solution (Sigma Aldrich) flowed through the channels followed by air blow dry. Then a library of DNA solutions, diluted in a mixture of DMSO and deionized water (v/v=1:2) with a final concentration of 267 μM, was flowed into each of the microfluidic channels. The solution-filled chip was placed in a desiccator to allow solvent (DMSO and water) to evaporate completely through the gas-permeable PDMS, leaving the DNA molecules behind. This evaporation process took 3 days to complete. Last, the PDMS elastomer was removed from the glass slide, and the barcode-patterned DNA was cross-linked to the glass surface by thermal treatment at 80°C for 4 hr. Residual crystals were removed by rapidly dipping the slide in deionized water. Each DNA barcode slide was validated before bonding to the single cell assay chip. A small area close to the edge was validated to check the DNA loading and uniformity. To do this, fluorescent Cy3-labeled complementary DNA cocktail in 1% Bovine Serum Albumin (BSA, Sigma Aldrich) in 1× PBS (Irvine Scientific) were hybridized for 1 hr. After washing three times with 1% BSA/PBS and PBS, the slide was dried by nitrogen gun and scanned by Axon GenePix 4400A. Under laser power of 15% and gain of 450, fluorescence intensity above 30,000 was acceptable for cytoplasmic protein detection at the single cell level. Figures S4A and S4B shows the effect of the additional PLL treatment on DNA loading and protein detection.

Cell sorting and preparation for the SCBC test. A solid tumor is composed of many different types of cells including immune cells, stromal cells, and cancer cells. In order to analyze the main characteristics of the cancer cells, it is required to sort out cancer cells, or specific subsets of cancer cells in a tumor sample. There are several challenges for cell sorting. First, the technique should be very specific, robust, and reproducible. Second, it should be able to handle small amount of sample. Third, cells after sorting should be healthy in order to provide representative information of the tumor. We chose to use magnetic bead-activated cell sorting (MACS) targeting EGFR cell surface marker. EGFR is one of the major cell surface markers for GBM which is over expressed in approximately 50–60% of glioblastoma (GBM) tumors (Heimberger et al., 2005). Cell sorting was carried out with Human EGF R/ErbB1^{+} Cancer Cells PlusCellect kit from R&D systems (Catalog # PLS1095), following the manufacturer's protocol. Typical cell number available from the mouse tissue sample ranges from 500,000 to 1,000,000 and the yield of the EGFR^{+} cell sorting is sample specific with a range of 60–70% for most of our cases. Cell variability after sorting is another critical issue, since primary cells are normally fragile. A short time (2 hr) incubation step on a laminin pre-coated petri dish was introduced to enable only healthy cells to attach to the plate and subsequently to be transferred to the SCBC test. The cell viability was greater than 95% after employing the surface plating step. Immunoblot analyses (Figure S4C) also confirmed that the additional short time culturing does not induce significant physiological changes in the primary cells. After 2 hr of incubation, dead suspended cells were removed by aspirating the media. Cells that attached to the surface were trypinized and re-suspended in the cell media (NeuroCult®-XF Proliferation Medium, STEMCELL Technologies, Inc.) at 1,000 cells/μL for loading to the SCBC.

Protocols of single cell proteomic assay. The procedures of using a SCBC for profiling intracellular proteins from single cells are as follows (Figure 3A):

a) Prior to cell loading, all microfluidic channels were blocked with a blocking buffer (3% BSA in 1× PBS) for 60 min.

b) Conversion of the DNA barcodes to capture antibody microarrays: a cocktail containing all DNA-antibody conjugates was introduced through the upper assay compartment of the SCBC and incubated at 37°C for 60 min. This transformed the DNA barcode microarrays into antibody microarrays for the subsequent surface-bound immunoassay. In parallel, a mixture of cell lysis buffer (5×, Cell Signaling, containing 20 mM Tris-HCl, 150 mM NaCl, 1 mM Na2EDTA, 1 mM EGTA, 1% Triton, 2.5 mM sodium pyrophosphate, 1 mM β-glycerophosphate, 1 mM Na3VO4 and 1 μg/ml leupeptin) with concentrated protease inhibitor (Roche) and phosphatase inhibitor cocktail 2 (Sigma Aldrich) were loaded into the lower lysis buffer reservoir while the valve 4 (Figure S4E-S4G) was kept closed by applying 20–22 psi constant pressure. The unbound conjugates were removed by flowing the washing buffer (3% BSA in PBS) for 10 min. The DNA-antibody conjugate solution (100 μL) was prepared by mixing all synthesized conjugates in the washing buffer with a final concentration of 10 μg/ml of each conjugate.

c) Cell loading: sorted and plated cells were dissociated with trypsin-EDTA (0.25%, ATCC), centrifuged at 4°C and suspended in Dulbecco's Modified Eagle's Medium (DMEM, American Type Culture Collection) with 1% fetal bovine serum (FBS) at a concentration of 1000 cells/μL. Before cell loading, the channels were briefly rinsed with medium. Cells were then loaded into the upper assay channels of the chip and the valve 3 (Figures S4E and S4F) was closed to compartmentalize the SCBC fluidic network into 310 isolated microchambers. Images of each chamber were recorded using a CCD camera, and used later for cell counting (Figure S4G).

d) On-chip cell lysis and protein measurement: after cell loading, the chip was placed on ice and the valve 4 was opened for on-chip diffusion of lysis buffer to the neighboring cell chambers (Figures S4E and S4F). To facilitate the diffusion process, the chip was tilted and 4.5 psi positive pressure was applied to lysis buffer reservoir before opening the valve 4. After 1 min, the pressure to the lysis buffer reservoir was released. Diffusion was completed in 15 min, after which valve 4 was closed and the chip was incubated on ice for another 15 min to complete the on-chip cell lysis. The chip was then incubated at room temperature with shaking for 2 hr to complete the capture of target proteins by antibody microarrays within the microchambers. Afterwards, the unbound cell lysate was quickly removed by flushing the washing buffer through the microchannels for 10 min.

e) Applying detection antibodies: a mixture of biotin-labeled detection antibodies was flowed into the assay channels of the chip for 60 min at room temperature to complete the sandwich immunoassay. The detection antibody solution contained biotinylated detection antibodies at concentrations specified in the insert of the ELISA kits (the concentration varies from lot to lot). Unbound detection antibodies were then flushed out by flowing the washing buffer for 10 min.

f) Fluorescence probe: Cy5 fluorescent dye-labeled streptavidin (eBioscience, 2 μg/ml) and the reference, Cy3-labeled complementary ssDNA (DNA code M/M' 50 nM) were combined in the washing buffer and flowed into the chip for 60 min to introduce the fluorescence probes for optical readout. Afterwards, the chip was washed by flowing the washing buffer for 60 min to remove unbound probes.

g) Rinse: the PDMS device was peeled from the DNA patterned glass slide, and was immediately dipped 3× each in the following solutions in order, 1X PBS, 0.5X PBS, deionized Millipore water. The slide was then dried by a VWR Miniarray microcentrifuge.

h) Optical readout: the slide was scanned by an Axon GenePix 4400A (Molecular Devices) at laser power 80% (635nm) and 10% (532nm), and at 2.5 μm/pixel resolution. Signals from two color channels (the green Cy3 and the red Cy5) were collected and the average fluorescence signals from each barcode were extracted by a custom MATLAB (The Mathworks) code for further analysis.

Statistical analysis of the single cell data. The SCBC readouts from the microchambers with a single cell were collected to form a data table. Each row of the table corresponds to a measurement of a panel of functional proteins from a single cell and each column contains digitized fluorescence intensities that provide readout of the levels of each of the assayed proteins. For getting enough statistical power, 60 or more single cell measurements were carried out for each test condition. Since the protein levels from a single tumor cell typically do not have a normal

distribution, statistical uniqueness is evaluated by two-tailed Mann-Whitney test for pairwise comparison and Kruskal-Wallis test for comparison among three or more groups.

Protein-protein Spearman's rank correlation coefficients can be directly calculated from single cell data. Protein correlation networks were generated by running the calculation through all the protein pairs in the panel (Figure 4A). The line weight defines the strength of the correlation and the size of the sphere that designates a given protein reflects the measured abundance of that protein. Bonferroni corrected (Curtin and Schulz, 1998) p-value was used to define the statistical significance level for the entire panel and only those significant correlations were shown in the networks.

AHC analysis was applied by XLSTAT software (Addinsoft) on the mean normalized single cell data extracted from control, responsive and resistant tumors respectively. The proximity among single cell observations was measured by the dissimilarity coefficients of Euclidian distance. Ward's minimum variance method was employed as a strategy to calculate the dissimilarity in order to minimize the total within-cluster variance and thus keep each clustered group as homogeneous as possible (Ward, 1963). The calculated dissimilarity coefficients were used as indices for quantifying the functional heterogeneity of the tumor.

PCA was carried out for single cell data from tumors at all three stages as well as the three clustered subgroups identified in control sample. Each column of the dataset was mean-centered and divided by the standard deviation to form a standardized dataset first. A normalized PCA was used to peel off layer after layer of systematic co-variations from the data, in terms of principal components (PCs). The correlations between functional protein levels and PCs were calculated to quantify the dominative protein pattern of the signaling network coordination and its response to external perturbations such as drug treatment.

Capture of EGFR, EGFRvIII positive cells by DNA Encoded Antibody Library (DEAL) and trypan blue staining. $EGFR^+$ and $EGFRvIII^+$ cells were sorted from GBM39 neurospheres by DEAL technology (Bailey et al., 2007). DEAL arrays were blocked with 1% BSA in PBS solution (g/mL) for 30 min, washed in PBS and deionized water and incubated with oligo-Cetuximab (Bristol-Myers) conjugate for 30 min, at 37°C. Single cell preparation of GBM39 cells, suspended in the culture medium, were applied to the array for 40 min, on ice. The DEAL arrays were then washed with BSA 0.1% in PBS (g/mL), a solution 1:2 of trypan blue in PBS (vol/vol) was applied on the captured cells that were then covered with a cover slip. Dead cells were visualized and counted as number of trypan blue positive cells, with a Nikon Eclipse TS100 scope.

Viability tests. Fifteen thousand of GBM39 cells were seeded in 12 well plates and, after 24 hr, treated with CC214-1 2 μM, U0126 5 μM, dasatinib 100 nM, for 24 hr. Cell viability and cell death were evaluated using Bio-Rad TC-20 cell counter. Representative images of the cells were taken using a Nikon Eclipse TS100 scope equipped with Canon S51S camera. One-way ANOVA and Student's T-test with Bonferroni correction were used to assess statistical significance (GraphPad Prism). The variation between the sample sets was similar and expressed as standard deviation.

Partial least square modeling (PLS) of IHC data. The digitized IHC data under different drug combinations was used to establish the explanatory metrics **X** (independent metrics) (Figure 6, Table S6). Prior to establish the corresponding dependent metrics **Y**, two characteristic terms that can be directly extracted from the tumor growth curves were introduced. One is the transitory growth rate (TGR) at the time of sacrifice, which is defined as the average percentage of tumor volume change per day of the last three time points available on the growth curves except for cases C+U DR, C+D DR and V2 where last two time points were used instead of three. The other term is the cell cycle measure (time constant τ) that can be extracted by fitting the growth curves (Figure 5A) with the exponential growth function. The tumor volume in the growth curves was modeled by the exponential growth function $V_t = V_0 + \varepsilon + V_0^{'} e^{t/\tau}$, where V_t is the normalized tumor volume over time. V_0 can be understood as the portion of the solid tumor that was not engaged in tumor growth and $V_0^{'}$ was the portion that was engaged in the tumor growth (Novak et al., 2001). $\varepsilon \sim N(0,\sigma)$ is an error term from a normal distribution with mean zero and SD σ. At the initial state (t=0), $V_t = V_0 + V_0^{'} = 1 - \varepsilon$. The application of effective drug combinations can significantly shut down the tumor progression and thus lead to large values of the cell cycle measure τ as expected (Table S6). Please note that the functional form used here is an oversimplified model without separately considering the initial/consistent cell death caused by the drugs or any phenotypical switch and emergence of resistance during the treatment. Only the single metric τ was used to roughly assess the drug effect since it still captures the essential information to disclose the independent signaling modes as discussed in the paper.

The PLS model was constructed in XLSTAT software (Addinsoft) according to the following iterative formulae (Martens and Martens, 2001):

$$\mathbf{w_a} = \text{first eigenvector of } (\mathbf{E'_{i-1}F_{i-1}F'_{i-1}E_{i-1}})$$

$$\mathbf{t_i} = \mathbf{E_{i-1}w_i}$$

$$\mathbf{E_i} = \mathbf{E_{i-1}} - \mathbf{t_i p'_i}$$

$$\mathbf{F_i} = \mathbf{F_{i-1}} - \mathbf{t_i q'_i}$$

$$\mathbf{p'_i} = (\mathbf{t'_i t_t})^{-1}\mathbf{t'_i E_{i-1}}$$

$$\mathbf{q'_i} = (\mathbf{t'_i t_t})^{-1}\mathbf{t'_i F_{i-1}}$$

where the $\mathbf{E_i}$ represents the residue of the ith PC of the explanatory metrics with the score vector $\mathbf{t_i}$, loading vector $\mathbf{p_i}$ while $\mathbf{F_i}$ represents the residue of the ith PC of the dependent metrics with score vector ti and loading vector $\mathbf{q_i}$. $\mathbf{w_i}$ is the loading weight that strikes a balance between modeling **X** and modeling **Y**. The prime represents the matrix transpose. The residue matrices $\mathbf{E_0}$ and $\mathbf{F_0}$ just contain the mean-centered **X-** and **Y-** variables. The regression coefficient matrix that leads out the functional form between **X** and **Y** can be calculated as $\mathbf{B_h} = \mathbf{W_h}(\mathbf{P'_h W_h})^{-1}\mathbf{Q'_h}$, where h is the number of PCs used in the model.

Eight observations (V1, C, D, U, C+D, D+U, C+U and C-R) were employed to establish the calibration phase of the model. The stability and predictive quality of the model were assessed by calculating Q^2cum index that involves the predicted residual sums of squares (PRESS) statistic and sum of squares of error (SSE) for a model with one less component (Allen, 1974).

$$Q^2cum(h) = 1 - \prod_{j=1}^{h} \frac{\sum_{k=1}^{n} PRESS_{kj}}{\sum_{k=1}^{n} SSE_{k(j-1)}}$$

PRESS statistic requires a leave-one-out cross-validation. The Q^2cum index measures the global contribution of the h first PCs to the predictive capacity of the model. As a result, the optimal number of PCs used in the model can be determined with respect to this index. The first two PCs yielded the highest Q^2cum index for this model and thus were employed in the subsequent calculations.

In the prediction phase, the established model was used to predict the TGR at sacrifice and cell cycle measure τ for the observations C+D DR, C+U DR and V2. The predicted values were compared against the observed values extracted from the growth curves and shown in Figure 5A. The good match between observation and prediction further validates the model reliability and stability.

In vitro tests and RIMChip experiments on the pcGBM2 cell line. pcGBM2 cells were sorted by anti-EGFR functionalized magnetic beads, treated in vitro for 48 hr with lapatinib at 2 mM, and loaded into SCBCs for functional proteomic analysis of single cells. Viability and proliferation after 2 days in vitro lapatinib treatment were assessed for both fresh $EGFR^+$ pcGBM2 cells and adapted $EGFR^+$ pcGBM2 cells (2000 nM lapatinib 2-day pretreatment on fresh $EGFR^+$ pcGBM2 cells was used to establish the adapted $EGFR^+$ cells). We started with two set of petri-dishes (3 repeats in each condition) with identical cell number: one for the control and the other for the lapatinib treatment. At the end of the 48 hr of the treatment, the cells were harvested, counted and re-plated with the identical cell number in two separate sets of dishes for another 48 hr of lapatinib treatment. One set represents the cells freshly treated with lapatinib and the other set represents the case of the second round treatment on the adapted cells derived from the first round of lapatinib treatment (Figure 7C). Consistently '48 hr DMSO then 48 hr lapatinib' shows decreased cell number (cell death). However, '48 hr lapatinib then 48 hr lapatinib' has an increased cell

number, which demonstrates that the cells will progress even faster after adapting to lapatinib. This is wholly consistent with our predictions from single-cell analysis.

To further validate the elevated aggressiveness of lapatinib treated cells, we performed another test with the RIMChip platform which offers an in vitro equivalent of ^{18}F-FDG PET scans by combining microchip/Beta particle camera. The RIMChip assay only requires about 100 cells/assay (each microchip supports 16 different assays) and yields metabolic assessments of drug responses (and response kinetics) in a few hr. This platform has been validated on both model and primary cells and tissues (Dooraghi et al., 2013; Wang et al., 2013). For the test, we treated EGFR$^+$ pcGBM2 cells with lapatinib for 0.5, 1, 1.5, and 2 hr and then loaded them to the RIMChip device with ^{18}F-FDG. After 30 min, remaining ^{18}F-FDG was washed off by PBS and the images were recorded by Beta particle camera (Figure S7B). The level of the glucose uptake was normalized by cell number to yield a quantitative comparison for all 5 conditions (Figure S7C). An elevated glucose consumption for lapatinib treated cells was observed within less than 1 hr, which is in line with the results from cell viability and proliferation assays.

To test the therapy combinations suggested by analyzing the change in signal coordination of pcGBM2 in response to lapatinib treatment, the cells were treated in vitro with 1 μM XL-765+100 nM trametinib for 60 hr. A significant cell killing with an accompanying reduction in the functional heterogeneity was observed.

Supplemental References

Allen, D. M. (1974). The relationship between variable selection and data agumentation and a method for prediction. Technometrics *16*, 125–127.

Curtin, F., and Schulz, P. (1998). Multiple correlations and Bonferroni's correction. Biol. Psychiatry. *44,* 775–777.

Fueger, B. J., Czernin, J., Hildebrandt, I., Tran, C., Halpern, B. S., Stout, D., Phelps, M. E., and Weber, W. A. (2006). Impact of animal handling on the results of ^{18}F-FDG PET studies in mice. J. Nucl. Med. *47*, 999–1006.

Heimberger, A. B., Suki, D., Yang, D., Shi, W., and Aldape, K. (2005). The natural history of EGFR and EGFRvIII in glioblastoma patients. J. Transl. Med. *3*, 38.

Hodgson, J. G., Yeh, R. F., Ray, A., Wang, N. J., Smirnov, I., Yu, M., Hariono, S., Siber, J., Feiler, H. S., Gray, J. W., et al. (2009). Comparative analyses of gene copy number and mRNA expression in glioblastoma multiforme tumors and xenografts. Neuro Oncol. *11,* 477–487.

Martens, H., and Martens, M. (2001). Multivariate analysis of quality : an introduction, (Chichester ; New York: Wiley).

Novak, B., Pataki, Z., Ciliberto, A., and Tyson, J. J. (2001). Mathematical model of the cell division cycle of fission yeast. Chaos *11*, 277–286.

Shin, Y. S., Ahmad, H., Shi, Q., Kim, H., Pascal, T. A., Fan, R., Goddard, W. A., 3rd, and Heath, J. R. (2010). Chemistries for patterning robust DNA microbarcodes enable multiplex assays of cytoplasm proteins from single cancer cells. Chemphyschem *11*, 3063–3069.

Verhaak, R. G. W., Hoadley, K. A., Purdom, E., Wang, V., Qi, Y., Wilkerson, M. D., Miller, C. R., Ding, L., Golub, T., Mesirov, J. P., et al. (2010). Integrated genomic analysis identifies clinically relevant subtypes of glioblastoma characterized by abnormalities in *PDGFRA*, *IHD1, EGFR*, and *NF1*. Cancer Cell *17,* 98–110.